Atomic Spectroscopy

Article

X-ray Fluorescence Analysis of Snow Cover Solid Phase for Investigation of Emissions by Aluminum Industry and Combined Heat and Power Complex

Alena A. Amosova,[a,*] Victor M. Chubarov,[a] Sergey N. Prosekin,[a,b] Ekaterina V. Kaneva[a,b]

[a] Vinogradov Institute of Geochemistry, Siberian Branch of the Russian Academy of Sciences, 1A Favorsky St., 664033 Irkutsk, Russia

[b] Irkutsk National Research Technical University, 83 Lermontov St., 664074, Irkutsk, Russia

Received: *May 29, 2023;* ***Revised:*** *July 03, 2023;* ***Accepted:*** *July 07, 2023;* ***Available online:*** *July 08, 2023.*

DOI: 10.46770/AS.2023.115

ABSTRACT: X-ray fluorescence method was proposed for a determination of major elements in samples of snow cover solid phase collected in the urban areas of the Irkutsk region near aluminum smelter and combined heat and power plant. The limitation of the analyzed sample mass, which in some cases does not exceed 50 mg, as well as the features of the elemental composition (high Al and low Si contents) require a special methodological approach to quantitative elemental analysis. Due to the lack of matrix-matched certified reference materials, the calibration set includes certified reference materials of igneous and sedimentary rocks as well as aluminum ore samples. Results of X-ray fluorescence method were compared with the results obtained by reference methods including atomic absorption, atomic emission and spectrophotometry methods. It showed that it is necessary to use samples of snow cover solid phase analyzed by reference methods as a calibration set for X-ray fluorescence analysis, which ensures the quantitative determination of major elements (Na, Mg, Al, Si, P, K, Ca, Ti, Mn and Fe). These elements are important for environmental pollution investigation. Al was discovered as a main pollutant produced by aluminum smelter, Si, Ca, Ti, Mn, and Fe - by combined heat and power plant.

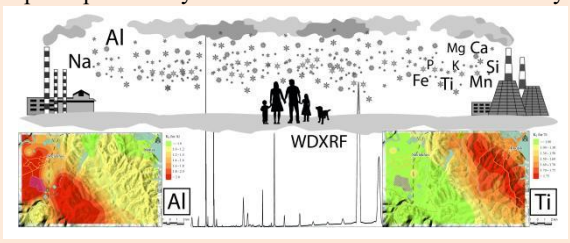

INTRODUCTION

The aluminum industry has significant environmental and health impact. Aluminum is a neurotoxic substance that has been found in high levels in the brain tissues of Alzheimer's disease, epilepsy, and autism patients, as well as premature infants and ones with renal failure, who are at the risk of developing the central nervous system and bone toxicity.[1] Besides alumina, air pollutions from aluminum smelters includes coke dust, particulate and gaseous fluorides, and sodium dioxide, as well as organic compounds.[2-5] Aluminum production facilities are often supplied by combined heat and power (CHP) plants which emit nitrogen dioxide, organic compounds, sulphur dioxide, as well as inorganic dust with toxic elements.[6] Air pollution control, identification of pollution areas and sources of potentially toxic elements, minimization of negative impacts on the environment and living organisms in the areas influenced by aluminum production and CHP facilities are current environmental problems. Fast and accurate methods for recognizing the effects of industrial emissions are required.

Snow cover is an important source of data for environmental pollution studies due to its accumulation of atmospheric dust particles.[7-21] During a snowfall, snow captures gaseous substances and solid particles suspended in the atmospheric air. When the snowfall stops, snow cover collects dry precipitation of particles and dust from the atmosphere. The study of the mineral and elemental composition of snow cover solid phase is important for a better understanding of the migration routes of pollutants and determining their impact on biological objects, including humans.

For analytical chemist, an analysis of snow cover solid phase is

not a simple task. Since the sample mass is limited and often does not exceed 50 mg, it is necessary to apply methods which do not require a large sample mass of the analyzed material, for example, inductively coupled plasma mass-spectrometry,[10,17,19,22] optic-emission spectrometry,[18,23] atomic emission[15,16,19] or atomic absorption analysis.[9,24] The X-ray fluorescence (XRF) method is widely used for the determination of elemental composition of various objects[25,26] for different studies, including environmental investigation.[27-34] However, despite the relatively low cost and high productivity, XRF method has not been applied for snow cover solid phase analysis. The experience of using X-ray methods in the analysis of this object is often limited to the study of individual particles by the electron probe microanalysis.[20,35-41] Common XRF techniques usually require a relatively large sample mass (from 500 mg), however a quantitative analysis of small sample mass is also possible.[42,43]

One of the problems in the study of snow cover solid phase is a specific phase composition of investigated samples. Wet chemistry methods based on the acid digestion procedure are almost free of influence of sample matrix, however the modern methods (including XRF) usually require matrix matched certified reference materials (CRMs) for quantitative analysis. There are no CRMs of snow cover solid phase, therefore specific techniques for the sample preparation are required. In contrast to the time-consuming acid leaching procedure, the fusion method can be used for XRF analysis to minimize the influence of the difference in phase composition between the analyzed and calibration samples.[44,45] Due to the development of facilities for a sample preparation to the XRF analysis it is possible to reduce the analyzed sample mass.[46-50] The limitations of the fusion sample preparation technique are: determination of volatile elements (S, F), which may be partially or completely lost during fusion process; determination of element content less than 0.1 wt. % due to the high degree of dilution with flux that significantly reduces the sensitivity of technique.

Other issues are specific elemental composition of investigated samples and, consequently, necessity for matrix effects correction. Two main approaches for the matrix effects correction in the XRF analysis are (1): the fundamental parameters (FP) model based on the physical model of X-ray radiation interaction with a sample and (2) the empirical influence coefficients (EIC) based on regression equations.[51-53] Application of FP requires knowledge of the bulk chemical composition of sample, while the construction of reliable empirical regression equations requires a large number of matrix-matched calibration samples. Due to the differences in contents and ratios of analytes in snow cover solid phase samples and the lack of matrix-matched CRMs, the selection of matrix effects correction method is also the important task.

This study presents the application of the XRF method with a fusion sample preparation procedure for the quantitative determination of major elements in snow cover solid phase sample with a limited mass. The purpose of this work is to assess environmental pollution of areas influenced by the aluminum production facilities and CHP plants emissions. This study also includes the selection of calibration samples and matrix effects correction approach in the conditions of the lack of matrix-matched CRMs and specific phase and elemental composition of industrial emissions.

EXPERIMENTAL

Instrumentation. Major components of emissions from the aluminum industry (Na, Al) and the CHP plants (Mg, K, Si, Ti, Ca) were considered as the elements of interest. Investigation was carried out using the equipment of the Center of isotopic and geochemical Research (Vinogradov Institute of Geochemistry, Siberian Branch of the Russian Academy of Sciences, Irkutsk, Russian Federation).[54] The measurements were performed using an S4 Pioneer wavelength-dispersive X-ray fluorescence spectrometer (Bruker AXS, Germany) equipped with Rh-anode X-ray tube and Soller optical scheme. Table 1 shows the conditions for measuring analytical lines: X-ray tube voltage and current, crystal monochromator (lithium fluoride LiF, pentaerythritol PET, synthetic multilayer crystal OVO-55), collimator and detector (SD – scintillation detector, GFPD – gas-flow proportional detector). The instrumental uncertainty is less than 0.3% rel. The measurement time for one sample was about 15 min.

Matrix effects correction was carried out using two methods, described in the Introduction section. The correction by FP method ("variable alphas" option of the spectrometer software) was applied using the following equation:

$$C_i^* = C_i \cdot (1 + \sum_{j \neq i}^{n} \alpha_{ij} \cdot C_j) \quad (1)$$

where C_i* – corrected content of analyte, C_j – content of the matrix element; α_{ij} - matrix correction coefficients.

The EIC method was applied using the following equation:

$$C_i^* = C_i \cdot (1 + \sum_{j \neq i}^{n} \alpha_{ij} \cdot I_j) \quad (2)$$

where I_j – intensity of the influencing element.

Table 1. Instrumental operating conditions for analytical lines

Analytical line	Voltage, kV / Current, mA	Crystal / collimator	Detector
Na Kα, Mg Kα	30 / 80	OVO-55 / 0.46°	GFPD
Al Kα, Si Kα, PKα	30 / 80	PET / 0.46°	GFPD
K Kα, Ca Kα, Ti Kα	50 / 40	LiF (200) / 0.23°	GFPD
Fe Kα, Mn Kα	50 / 40	LiF (200) / 0.23°	SD

Notes: SD—scintillation detector, GFPD—gas-flow proportional detector.

Cluster analysis (CA) and principal component analysis (PCA) has been applied using Statistica 12 software. Maps were prepared in the QGIS 3.16 software. Spatial data processing algorithms of the SAGA GIS 7 integrated into QGIS software were used to build the spatial distribution of elements.

Materials and sample preparation. Samples of the snow cover solid phase were collected from Irkutsk region urbanized territories: Irkutsk and Shelekhov cities and their suburbs, where the main sources of high levels of air pollution are the Irkutsk Aluminum Smelter (including CHP plant, silicon, and cable production) and the Novo-Irkutsk CHP plant. The sampling scheme was drawn up considering the physical and geographical conditions, including the wind rose, the location of industrial enterprises and the terrain (Fig. 1). Samples were collected at the end of the stable snow cover season during the period of its maximum accumulation before the onset of thawing (late February and early March, from 2020 to 2022). Sampling was carried out to the entire depth of the snow layer, except for a 5-cm layer above the soil, using special polyvinyl samplers in plastic bags, while measuring the area and depth of the pit.

Fig. 1 Map-scheme of the study area.

Snow samples were thawed at room temperature, and the melt water was filtered. The mass of obtained solid samples varied from 0.1 g to 2.0 g. According to the XRD data, collected samples consist of oxide phases containing aluminum and iron, presumably of technogenic origin: mainly corundum, mullite, and hematite, as well as natural minerals (quartz, anorthite, muscovite, phologopite). According to the previous studies using electron probe microanalysis, samples collected from the same area also could contain microparticles of aluminum oxides and carbides and metal spherules of iron sulfides.[35-37,39] Fig. 2 shows spectra of snow cover solid phase samples collected near aluminum smelter (a), CHP plant (b) and out of investigated area (c). The most intense lines are related with the presence of high Al (1.5 keV), Fe (6.4 keV), Ca (3.7 keV) and Si (1.7 keV) content. These major elements were considered as potential pollutants.

Fig. 2 X-ray fluorescence spectrum of snow cover solid sample collected near aluminum smelter (a), CHP plant (b) and out of investigated area (c).

Figure 1 also shows 12 samples (blue dots) chosen for XRF investigation and analyzed by reference methods (Table 2). These samples have the maximum mass and therefore they were considered as most polluted. Ten samples were collected near aluminum smelter and two samples – near Novo-Irkutsk CHP plant. The elemental composition of the samples is presented in supplementary files (Table S1).

The phase composition of the samples was studied by X-ray powder diffractometry (XRD) using a D8 Advance powder diffractometer (Bruker AXS, Germany). The approved analytical methods of atomic emission spectroscopy (Kolibri-2 multichannel spectrometer, VMK-Optoelektronika, Russia), atomic absorption spectroscopy (M403 spectrometer, Perkin-Elmer, USA) and spectrophotometry (SF-56 spectrophotometer, OKB Spectr, Russia) were used as reference methods.

Obtained results were processed by CA and PCA to classify samples with different composition. The “Eigenvalues scree Plot” was used to determine two optimal principal components. Calculations showed that the first two principal components represent 86% of the total variance (factor 1 = 70.6%, factor 2 = 15.4%). Score and loading scatter plots were constructed in

Table 2. Analysis of snow cover solid phase samples by reference methods

Compound	Concentration range, wt. %	Method
Na_2O	0.10-1.79	Atomic emission spectroscopy
K_2O	0.12-3.02	
MgO	0.11-1.99	Atomic absorption spectroscopy
Al_2O_3	28.54-73.07	
CaO	0.51-5.26	
MnO	0.03-0.10	
Fe_2O_3	0.36-6.40	
SiO_2	6.63-48.26	Spectrophotometry
P_2O_5	0.06-0.20	
TiO_2	0.07-0.77	
Loss on ignition (LOI)	5.22-21.53	Gravimetry

Fig. 3 PCA results based on the elemental composition of snow cover solid phase samples obtained by reference methods: score scatter plot (a) and loading scatter plot (b) for two factors.

projections on the first and the second factors (Fig. 3) to study the relationship of all variables. The most significant variables for the first factor are Al, Si, Ti, Mn, and Fe. The second factor divides the samples by the content of Na.

The score scatter plot shows a clear differentiation of samples collected near Novo-Irkutsk CHP plant (samples 1 and 4) and Irkutsk aluminum smelter (other 10 samples). The main difference in chemical composition caused by the variations of Na and K or Al and LOI (including F and C) contents in aluminum smelter emissions and Ca content in CHP plant emissions. The data obtained showed that sources of pollution are various in different fields of investigated area. According to a visual assessment of PCA graphs, 12 samples were divided into two groups.

Calibration samples. The calibration set was selected according to the ranges of elements' contents determined for the samples of snow cover solid phase by reference methods (Table 2). We used CRMs of igneous and sedimentary rocks produced by the Vinogradov Institute of Geochemistry (Irkutsk, Russia): SDU-1 (dunite), SKD-1 (quartz diorite), SGD-2 (gabbro), SG-3 and SG-4 (granites), GBPg-1 (garnet-biotite plagiogneiss); West Siberian Testing Center (Yekaterinburg, Russia): SO-12 (granite); International Association of Geoanalysts (IAG): DBC-1 (GeoPT-33, soil), UoKLoess (GeoPT-13, loess) and SdAR-1 (GeoPT-31, modified river sediment); CRMs of aluminum raw materials produced by Research Institute of Applied Physics (Irkutsk, Russia): SB-1 and SB-2 (bauxite), SNS-1 (nepheline ore) and The Center for Mineral Technology (CETEM, Brazilia): BXSP-1, BXMG-1, BXMG-3, BXMG-5, BXPA-2 and BXGO-1 (bauxites). CRMs contain high aluminum concentrations due to the presence of minerals—aluminum hydroxides (boehmite, diaspore, gibbsite) and aluminum silicates (kaolinite, zeolite). The data on elemental and phase composition was taken from GeoREM database (*http://georem.mpch-mainz.gwdg.de*), websites of IAG (*https://www.geoanalyst.org/geopt)* and CETEM (*https://cetem.gov.br/antigo/crm*).

Calibration set and analyzed samples were preliminarily calcined for 4 hours in a muffle furnace at a temperature of 950 °C. Because elements' contents are usually increasing during calcination (when LOI values related to water and carbon compounds), we recalculated elements' contents to calcined samples using certified (for CRMs) and determined by gravimetric technique (for collected samples) LOI values. Calcined samples with a mass of 110 mg were fused with 1.1 g of lithium metaborate (Merck) with the addition of seven drops of a 4% LiBr solution in platinum crucibles in a TheOX electric furnace (Claisse, Canada) at a temperature of 1050 °C.[46,47] The melt was poured onto platinum substrates and glass discs with a diameter of 10—12 mm were formed.

Validation. To assess the difference between results obtained by the XRF method and reference methods, the standard deviation (SD) value was calculated as follows:

$$SD = \sqrt{\frac{\sum (C_{XRF} - C_{ref})^2}{n}} \quad (3)$$

where C_{XRF} and C_{ref} - concentrations obtained by XRF and reference methods, n - the number of samples. The relative standard deviation (RSD) was calculated as follows:

$$RSD = \sqrt{\frac{\sum (\frac{C_{XRF} - C_{ref}}{C_{ref}})^2}{n}} \quad (4)$$

To compare the results obtained by XRF and reference methods, Z-score was calculated as follows:[55,56]

$$Z = \frac{C_{XRF} - C_{ref}}{0.02 \cdot (C^{ref})^{0.8495}} \quad (5)$$

Assessment of pollution level. The assessment of the pollution level was performed by a comparison of the obtained results with the values accepted as a regional background. As this study deals with a unique geosystem of the Baikal region, the methodology

Table 3. Characteristics of calibration curves (wt. %)

Compound	I				II				LOD
	Range	RMS			Range	RMS			
		Without correction	FP	EIC		Without correction	FP	EIC	
Na_2O	0.04-2.41	0.11	0.11	0.11	0.11-1.96	0.08	0.08	0.05	0.04
MgO	0.10-2.31	0.06	0.05	0.03	0.13-2.18	0.05	0.05	0.05	0.03
Al_2O_3	19.10-90.60	2.50	2.45	1.08	30.45-88.33	2.57	2.36	0.69	0.15
SiO_2	6.89-58.82	0.95	0.93	0.46	8.01-51.69	0.71	0.71	0.58	0.07
P_2O_5	0.04-0.38	0.02	0.02	0.01	0.07-0.24	0.01	0.01	0.01	0.01
K_2O	0.01-3.73	0.06	0.06	0.06	0.15-3.28	0.03	0.03	0.03	0.01
CaO	0.22-7.39	0.07	0.08	0.06	0.62-5.51	0.10	0.10	0.07	0.01
TiO_2	0.02-0.87	0.03	0.03	0.03	0.08-0.78	0.02	0.02	0.02	0.02
MnO	0.02-0.28	0.012	0.009	0.009	0.04-0.11	0.005	0.005	0.003	0.005
Fe_2O_3	1.04-9.51	0.27	0.21	0.21	0.67-8.41	0.17	0.15	0.15	0.02

Notes: FP—fundamental parameters model, ECI—empirical influence coefficients method, LOD—limit of detection, RMS—root mean square.

for determining the local background parameters differs from the generally accepted ones. Several background samples are taken outside the study area, 20 km away from the emission source. This is a background area identical to the emission source area in terms of climatic parameters, geological structure, relief, and soil cover. The sampling location satisfies the minimum urbanization of the surrounding area. After statistical processing of the data, the content of the elements, conventionally taken as the background, was determined (presented in supplementary files, Table S3). Pollution level was assessed using coefficients of elements' concentrations:

$$K_c = \frac{C}{C_b} \quad (6)$$

where C – content of element in sample; C_b – background content of element.

RESULTS AND DISCUSSION

Since the phase composition of the calibration set and analyzed samples is significantly different, and the calibration set does not include matrix-matched CRMs, we considered several options for constructing calibration equations.

I. CRMs listed in the Experimental section were used as a calibration set. For each analyte, the calibration range was chosen based on the data obtained by reference techniques for samples in Table 1. The number of calibration samples varied from nine to seventeen. Matrix effects were corrected in two ways: FP method (eq. (1)) or EIC method (eq. (2)). For EIC method the main elements of emission (Al, Si, Fe) were considered as influencing elements. The information about calibration samples and influencing elements are presented in supplementary files (Table S2).

II. According to the PCA (Fig. 3), samples of snow cover solid phase analyzed by the reference techniques were divided into two groups. Two samples (10 and 12), collected near aluminum smelter, and one sample (4), collected near Novo-Irkutsk CHP plant were chosen for a validation. Other nine samples were used as a calibration set. Two methods for matrix effects correction were also considered.

Table 3 shows the ranges of analytes, limit of detection (LOD) and root mean square (RMS) values, characterizing scatter of points relative to calibration curves (n varied from 9 to 17) and calculated as:

$$\mathrm{RMS} = \sqrt{\frac{\sum (C^{cert} - C^{XRF})^2}{n}} \quad (7)$$

where C^{cert} – certified content in CRM, C^{XRF} – content in CRM calculated using calibration curve.

EIC method allows to significantly reduce the RMS value for aluminum and silicon compared to the theoretical correction, while for the other elements the difference is insignificant. To assess the accuracy and select the optimal calibration equation, three test samples were analyzed according to the variants of equations I and II. Results were recalculated to uncalcined sample. Results are presented in supplementary files (Table S4). Table 4 shows obtained values of SD, RSD (n=3) and Z-score.

According to the data given in Table 4, the use of snow cover solid phase samples analyzed by reference techniques as a calibration set enables to reduce the error for Al, Si, and Ca by more than 3 times and for Mg by more than 2 times, while the accuracy is almost the same for Na, K, Ti. According to the Z-criterion, the results of the determination of Al, Si, and Fe in all three samples by the reference methods (II) can be accepted as satisfactory ($|Z|<2$). For XRF analysis using CRMs (I), the results

Table 4. Comparison of two calibration sets for XRF analysis

No.		Na_2O	MgO	Al_2O_3	SiO_2	P_2O_5	K_2O	CaO	TiO_2	MnO	Fe_2O_3
	C_{ref}, wt. %	0.14	1.48	29.98	48.26	0.16	0.83	5.26	0.77	0.09	7.38
4	Z_I	-1.20	-9.68	1.96	-3.88	-5.62	-2.79	4.05	-2.53	-2.70	2.78
	Z_{II}	2.69	-4.51	0.29	-1.14	0.40	-0.31	0.67	-2.74	5.07	0.26
	C_{ref}, wt. %	1.17	1.58	36.37	37.75	0.15	2.12	2.35	0.45	0.09	4.78
10	Z_I	-2.70	-7.55	2.03	-1.56	-6.01	1.79	0.02	-0.18	-15.68	-5.11
	Z_{II}	-0.13	-0.82	-1.12	0.62	0.06	3.08	0.27	2.09	-7.65	-1.89
	C_{ref}, wt. %	0.82	0.60	59.01	15.17	0.08	0.42	1.73	0.20	0.04	1.89
12	Z_I	3.57	3.16	2.71	-2.40	-9.02	-0.36	-2.24	-2.90	-17.09	1.41
	Z_{II}	2.37	3.13	-0.08	-0.48	-2.64	0.84	-0.25	1.57	2.84	0.94
SD_I		0.05	0.20	1.19	1.30	0.02	0.05	0.20	0.02	0.03	0.29
SD_{II}		0.02	0.08	0.28	0.39	0.01	0.07	0.03	0.03	0.01	0.09
RSD_I		5.55	13.88	2.56	3.28	19.73	3.82	4.35	5.24	41.54	5.47
RSD_{II}		5.03	6.34	0.78	0.92	4.49	3.38	0.72	4.86	16.21	2.00

Fig. 4 Results of CA of elemental composition of snow cover solid phase samples.

Table 5. Minimal, maximum, and average values of elements concentration coefficients, percentage of polluted samples

	K_c^{min}	K_c^{max}	$K_c^{average}$	$K_c^{\%}$
Na	0.2	1.9	0.4	4
Mg	0.1	1.1	0.6	3
Al	0.9	2.8	1.5	92
Si	0.1	1.2	0.8	47
P	0.1	1.4	0.6	1
K	0.1	3.7	0.9	13
Ca	0.2	2.0	1.0	51
Ti	0.1	1.8	1.1	57
Mn	0.1	1.7	0.9	51
Fe	0.2	6.1	1.1	60

can be considered as doubtful only for Al ($2<|Z|<3$). In total, out of thirty samples, the results for only eight samples can be considered as satisfactory and for other eight samples as doubtful obtained by equations I. Using of the calculation by equations II , the results for twenty samples can be accepted as satisfactory and for six samples as doubtful. Thus, it is preferable to use the samples for a calibration purposes preliminary analyzed by approved methods. Results of quantitative XRF analysis were used for further assessment of pollution level in the investigated area. According to the proposed methodology, 150 samples were collected in the area near the Irkutsk aluminum smelter and Novo-Irkutsk CHP plant (points of sampling are shown in Fig. 1) and analyzed from 2020 to 2022. Fig. 4 shows results of CA for 72 samples collected in 2020.

As can be seen from Fig. 4, the contents of LOI, Al and Na are strictly correlated with each other, which corresponds to the studies,[4,5] established that the main (with content more than 10 wt. %) components of gas and dust emissions from Irkutsk Aluminum smelter are aluminum oxide, carbon, cryolite Na_3AlF_6 and chiolite $Na_5Al_3F_{14}$. This suggests a technogenic source of these elements. A closely related association of Mn, Ca, Ti, Si, K, and Mg probably characterizes emissions from the CHP plants. Table 5 shows ranges and average values of elements concentration coefficient as well as percentage of polluted (K_c>1) samples ($K_c^{\%}$).

As can been seen from the Table 5, there is no significant pollution of snow cover solid phase by Na, Mg, and P (K_c values was more than 1 only for one sample for P, two samples for Mg, and 3 samples for Na). Even though Na, along with Al, is one of the main components of emissions from the aluminum industry, only 4% of samples contain Na, exceeding the background values. The reason is that some elements can be completely dissolved during the sample preparation procedure and remain in the water after filtration. According to a study conducted for other aluminum smelter located in same region,[57] only about 10% of Na remains in snow cover solid phase, while for Al this value reaches 100%. Fig. 5 shows a spatial distribution of Al in snow cover solid phase samples in the suburban areas of Shelekhov and Irkutsk cities.

High values of K_c for Al related with Irkutsk aluminum smelter emissions, which settling on the Shelekhov city territory.

Fig. 5 Spatial distribution of Al in snow cover solid phase samples in the suburban areas of Shelekhov and Irkutsk cities.

Fig. 6 Spatial distribution of Si (a), K (b), Ca (c), Ti (d), Mn (e) and Fe (f) in snow cover solid phase samples in the suburban areas of Shelekhov and Irkutsk cities.

Quantification of Al in snow cover solid phase by the XRF method allows us to clearly assess the pollution areas and find the level of pollution by aluminum industry as high. The obtained distribution is in a good agreement with the distribution of F obtained for investigated area.[21] Spatial distribution of Na is presented in supplementary materials (Fig. S1).

Figure 6 shows the spatial distribution for other elements (Si, K, Ca, Ti, Mn, Fe) in snow cover solid phase samples in the suburban areas of Shelekhov and Irkutsk cities.

High values of K_c for Si, Ca, Fe, Mn, and Ti related with the CHP plant emission, settling on the Irkutsk city territory according to the wind rose. As can be seen for Fe distribution (Fig. 6f), extremal values of K_c are observed near aluminum smelter, where several facilities (cable production, asphalt plant) are located. This anomaly has also been observed for Mn for several years and can be associated both with operation of CHP plant or city heaters, and with the repair of railways. High K_c values for Ca and K may be associated with anti-icing treatment of roads. Thus, the proposed method allows to assess the degree of industrial pollution of the snow cover.

CONCLUSION

The proposed XRF method allows to quantify major elements (Na, Mg, Al, Si, P, K, Ca, Ti, Mn, Fe) in samples of snow cover polluted by industrial emissions. The work showed that the construction of calibration curves should be carried out using the preliminary analyzed samples of snow cover solid phase by reference methods. The RSD values, presenting the comparison of XRF and certified techniques (atomic absorption spectrometry, spectrophotometry, atomic emission spectrometry) data, did not exceed 1 rel. % for Al, Si, Ca, 2 rel. % for Fe, and 7 rel. % for other elements (except for Mn, which content did not exceed 0.1% in the samples). Spatial distribution of elements in the investigated area allowed us to discover the main pollution elements produced by the aluminum smelter (Al) and CHP plant (Si, Ca, Ti, Mn, Fe). XRF method has the advantage of being simple, cheap, and fast method that can be used for studying environmental pollution.

ASSOCIATED CONTENT

The supporting information (Tables S1−S4, and Fig S1) is available at www.at-spectrose.com/as/home

AUTHOR INFORMATION

Alena Amosova received her specialty engineer-nanotechnologist in 2014 from the Irkutsk State Technical University, she graduated from the postgraduate course in 2018 in the direction of Chemical Sciences (focus of Analytical Chemistry) and PhD in 2019 from the Vinogradov Institute of Geochemistry (Siberian Branch of the Russian Academy of Sciences). She is a researcher at laboratory of X-ray methods of analysis in the Vinogradov Institute of Geochemistry. Her major research interests are X-ray fluorescence analysis of geological objects (bottom and peat sediments, rocks, ores, rocks), geochemistry, application of X-ray spectrometry for paleoclimatic studies. She has been working in DIMA (Developing Innovative Multi-Proxy Analyses) Network.

Corresponding Author

* A. A. Amosova

Email address: alena_amosova@mail.ru

Notes

The authors declare no competing financial interest.

ACKNOWLEDGMENTS

The research was performed by the governmental assignment in terms of project No. 0284-2021-0005 using the equipment of the Center of isotopic and geochemical Research, Vinogradov Institute of Geochemistry, Siberian Branch of the Russian Academy of Sciences, Irkutsk, Russian Federation with the financial support of the Grant for Young Candidates of Sciences (MK-2709.2022.1.5). Images for the Graphical Abstract were taken from https://publicdomainvectors.org/. We thank Artem Maltsev for language editing and Maria Kushnarenko for preparing the Graphic Abstract.

REFERENCES

1. R. H. Alasfar and R. J. Isaifan, *Environ. Sci. Pollut. R.*, 2021, **28**, 44587–44597. https://doi.org/10.1007/s11356-021-14700-0
2. N. P Cheremisinoff and P. F. Rosenfeld, Pollution and Pollution Prevention in: Handbook of Pollution Prevention and Cleaner Production: Best Practices in the Agrochemical Industry. Norwich, Elsevier, 2011, 25–79. https://doi.org/10.1016/b978-1-4377-7825-0.00002-9
3. D. Brough and H. Jouhara, *Int. J. Thermofluids*, 2020, **1–2**, 100007. https://doi.org/10.1016/j.ijft.2019.100007
4. N. V. Golovnyh, V. A. Verhozina, E. V. Verhozina, and A. S. Safarov, *Industrial Ecology*, 2013, 3, 57–63. https://elibrary.ru/item.asp?id=20192442
5. N. V. Golovnykh, V. A. Bychinskii, L. M. Filimonova, and O. M. Glazunov, Inzheneraya Geologiya, Gidrogeologiya, Geokriologiya, 2014, **3**, 224–232. https://elibrary.ru/item.asp?id=21633458
6. P. Córdoba, Emissions of Inorganic Trace Pollutants from Coal Power Generation in Air Pollution - Monitoring, Quantification and Removal of Gases and Particles. London, IntechOpen, 2018. https://doi.org/10.5772/intechopen.79918
7. M. Dinu, T. Moiseenko, and D. Baranov, *Atmosphere-Basel*, 2020, **11**, 462. https://doi.org/10.3390/atmos11050462
8. L. M. Filimonova, A. V. Parshin, and V. A. Bychinskii, *Russ. Meteorol. Hydrol.*, 2015, **40**, 691–698. https://doi.org/10.3103/S1068373915100076
9. T. R. Walker, S. D. Young, P. D. Crittenden, and H. Zhang, *Environ. Pollut.*, 2003, **121**, 11–21. https://doi.org/10.1016/S0269-7491(02)00212-9
10. M. Szwed and R. Kozłowski, *Atmosphere-Basel*, 2022, **13**, 409. https://doi.org/10.3390/atmos13030409
11. A. V. Talovskaya, E. A. Filimonenko, E. G. Yazikov, and L. V. Nadeina, Proc. SPIE 9292, 20th International Symposium on Atmospheric and Ocean Optics: Atmospheric Physics, 2014, 929236. https://doi.org/10.1117/12.2075597
12. L. Lisetskaya and S. Shayakhmetov, *Public health and life environment ─PH&LE*, 2021, **3**, 41–46 . https://doi.org/10.35627/2219-5238/2021-336-3-41-46
13. A. V. Talovskaya, V. D. Kirina, V. V. Litay, T. S. Shakhova, D. A. Volodina, and E. G. Yazikov, *Pure Appl. Chem.*, 2021, **94**, 249–256. https://doi.org/10.1515/pac-2021-0313
14. D. A. Volodina, A. V. Talovskaya, A. Yu. Devyatova, A. V. Edelev, and E. G. Yazikov, *Pure Appl. Chem.*, 2021, **94**, 269–274. https:/doi.org/10.1515/pac-2021-0315
15. V. I. Grebenshchikova, N. V. Efimova, and A. A. Doroshkov, *Environ. Earth Sci.*, 2017, **76**, 712–721. https://doi.org/10.1007/s12665-017-7056-0
16. I. V. Galitskaya and N. A. Rumyantseva, *Ann. Glaciol.*, 2012, **53**, 23–26. https://doi.org/10.3189/2012AoG61A009
17. E. Yakovlev, A. Druzhinina, E. Zykova, S. Zykov, and N. Ivanchenko, *Pollution*, 2022, **8**, 1274–1293. https://doi.org/10.22059/POLL.2022.341500.1438
18. D. N. Kurbakov, V. K. Kuznetsov, H. V. Sidorova, N. V. Andreeva, A. V. Sarukhanov, and V. E. Nushtaeva, *J. Phys.: Conf. Ser.*, 2020, **1701**, 012017. https://doi.org/10.1088/1742-6596/1701/1/012017
19. D. Moskovchenko, R. Pozhitkov, A. Zakharchenko, and A. Tigeev, *Minerals−Basel*, 2021, **11**, 709–729. https://doi.org/10.3390/min11070709
20. D. Gregurek, F. Melcher, V. A. Pavlov, C. Reimann, and E. F. Stumpfl, *Miner. Petrol.*, 1999, 65, 87–111. https://doi.org/10.1007/BF01161578
21. S. N. Prosekin, A. A. Amosova, V. M. Chubarov, and V. A. Bychinsky, *Geosphere Research*., 2023 (in Russian) (in press)
22. N. A. Osipova, K. A. Filimonenko, A. V. Talovskaya, and E. G. Yazikov, *Hum. Ecol. Risk Assess.*, 2015, **21**, 1664–1685. https://doi.org/10.1080/10807039.2014.972912
23. O. Akba and F. Aydin, *At. Spectrosc.*, 2013, **34**, 48–52. https://doi.org/10.46770/AS.2013.02.002
24. V. V. Kokovkin and V. F. Raputa, *Interexpo GEO-Siberia*, 2020, **4**, 49–56. https://doi.org/10.33764/2618-981X-2020-4-1-49-56
25. A. G. Revenko, *X-Ray Spectrom.*, 2002, **31**, 264–273. https://doi.org/10.1002/xrs.564
26. T. D. T. Oyedotun, *Geol. Ecol. Landsc.*, 2018, **2**, 148–154. https://doi.org/10.1080/24749508.2018.1452459
27. E. Marguí, I. Queralt, and E. de Almeida, *Chemosphere*, 2022, **303**, 135006. https://doi.org/10.1016/j.chemosphere.2022.135006
28. S. Piórek, *J. Radioanal. Nucl. Chem.*, 1980, **58**, 373–380. https://doi.org/10.1007/BF02533809
29. V. Chubarov, T. Cherkashina, A. Maltsev, E. Chuparina, A. Amosova, and S. Prosekin, *Agronomy*, 2022, **12**, 454–472. https://doi.org/10.3390/agronomy12020454
30. W. P. Linak, J. -I. Yoo, S. J. Wasson, W. Zhu, J. O. L. Wendt, F. E. Huggins, Y. Chen, N. Shah, G. P. Huffman, and M. I. Gilmour, *P. Combust. Inst.*, 2007, 31, 1929–1937. http://doi.org/10.1016/j.proci.2006.08.086
31. F. Mazzei, A. D' Alessandro, F. Lucarelli, S. Nava, P. Prati, G. Valli, and R. Vecchi, *Sci. Total Environ.*, 2008, **401**, 81–89. http://doi.org/10.1016/j.scitotenv.2008.03.008
32. U. E. A. Fittschen and G. Falkenberg, *Spectrochim. Acta B*, 2011, **66**, 567–580. http://doi.org/10.1016/j.sab.2011.06.006
33. F. Adams, *EPJ Web Conf.*, 2010, **9**, 165–180. http://doi.org/10.1051/epjconf/201009013
34. F. Bilo, L. Borgese, A. Wambui, A. Assi, A. Zacco, S. Federici, D. M. Eichert, K. Tsuji, R. G. Lucchini, D. Placidi, E. Bontempi, and L. E. Depero, *J. Aerosol Sci.*, 2018, **122**, 1–10.

http://doi.org/10.1016/j.jaerosci.2018.05.003

35. O. Yu. Belozerova, A. L. Finkelshtein, and L. A. Pavlova, *Micron*, 2003, **34**, 49–55. https://doi.org/10.1016/S0968-4328(02)00056-2
36. O. Yu. Belozerova, G. P. Koroleva, and L. A. Pavlova, Analitika i kontrol’ [Analytics and Control], 2002, **6**, 477–484. https://elar.urfu.ru/handle/10995/57274
37. O. Yu. Belozerova, A. L. Finkel'shtein, L. A. Pavlova, and V. G. Barankevich, *J. Anal. Chem.*, 1999, 54, 24–27 (in Russian).
38. M. S. Kholodova, M. V. Pastukhov, V. A. Bychinsky, S. N. Prosekin, and O. Yu. Belozerova, *Bull. Tomsk Polytech. Univ. Geo Assets Eng.*, 2022, 333, 219–230 (in Russian). https://doi.org/10.18799/24131830/2022/9/3687
39. L. A. Pavlova, O. Yu. Belozerova, and L. F. Paradina, *J. Anal. Chem.*, 2002, **57**, 407–414. https://doi.org/10.1023/A:1015405424136
40. L. A. Pavlova, O. Yu. Belozerova, and L. Ph. Paradina, *X-Ray Spectrom.*, 2002, **31**, 239–246. https://doi.org/10.1002/xrs.574
41. L. A. Pavlova, L. Ph. Paradina, and O. Yu. Belozerova, *Geostand. Geoanal. Res.*, 2001, **25**, 333–344. https://doi.org/10.1111/j.1751-908X.2001.tb00610.x
42. M. F. Gazulla, S. Vicente, M. Orduña, and M. J. Ventura, *X-Ray Spectrom.*, 2012, **41**, 176–185. https://doi.org/10.1002/xrs.2381
43. F. De Vleeschouwer, V. Renson, P. Claeys, K. Nys, and R. Bindler, *Geoarchaeology*, 2011, **26**, 440–450. https://doi.org/10.1002/gea.20353
44. M. T. Haukka and I. L. Thomas, *X-Ray Spectrom.*, 1977, **6**, 204–211. https://doi.org/10.1002/xrs.1300060410
45. P. K. Harvey, D. M. Taylor, R. D. Hendry, and F. Bancroft, *X-Ray Spectrom.*, 1973, 2, 33–44. https://doi.org/10.1002/xrs.1300020109
46. A. A. Amosova, S. V. Panteeva, V. V. Tatarinov, V. M. Chubarov, and A. L. Finkelshtein, Analitika i kontrol’ [Analytics and Control], 2015, **19**, 130-138. https://doi.org/10.15826/analitika.2015.19.2.009
47. A. A. Amosova, S. V. Panteeva, V. M. Chubarov, and A. L. Finkelshtein, *Spectrochim. Acta B*, 2016, **122**, 62–68. https://doi.org/10.1016/j.sab.2016.06.001
48. A. A. Amosova, V. M. Chubarov, G. V. Pashkova, A. L. Finkelshtein, and E. V. Bezrukova, *Appl. Radiat. Isotopes*, 2019, **144**, 118–123. https://doi.org/10.1016/j.apradiso.2018.11.004
49. K. Nakayama, S. Ichikawa, and T. Nakamura, *X-Ray Spectrom.*, 2011, 41, 16–21. https://doi.org/10.1002/xrs.1371
50. D. -S. Xue, H. -C. Tian, D. -P. Zhang, Y. -H. Liu, J. -F. Sun, S. -T. Wu, S. -K. Liu, S. Guo, and B. Wan, *Spectrochim. Acta B*, 2022, **193**, 106433. https://doi.org/10.1016/j.sab.2022.106433
51. J. Kawai, K. Yamasaki, R. Tanaka, Fundamental Parameter Method in X-Ray Fluorescence Analysis in Encyclopedia of Analytical Chemistry: Applications, Theory and Instrumentation. Hoboken, John Wiley & Sons, 2019. https://doi.org/10.1002/9780470027318.a9666
52. V. P. Afonin, A. L. Finkelshtein, V. J. Borkhodoev, and T. N. Gunicheva, *X-Ray Spectrom.*, 1992, **21**, 69–75. https://doi.org/10.1002/xrs.1300210205
53. D. K. G. De Boer, J. J. M. Borstrok, A. J. G. Leenaers, H. A. Van Sprang, and P. N. Brouwer, *X-Ray Spectrom.*, 1993, **22**, 33–38. https://doi.org/10.1002/xrs.1300220109
54. S. Yu. Skuzovatov, O. Yu. Belozerova, I. E. Vasil’eva, O. V. Zarubina, E. V. Kaneva, Yu. V. Sokolnikova, V. M. Chubarov, and E. V. Shabanova, *Geodyn. Tectonophys.*, 2022, **13**, 0585 (in Russian). https://doi.org/10.5800/GT-2022-13-2-0585
55. M. Thompson, P. C. Webb, and P. J. Potts, *Geostand. Geoanal. Res.*, 2015, **39**, 433–442. https://doi.org/10.1111/j.1751-908X.2014.00343.x
56. W. Horwitz, *Anal. Chem.*, 1982, **54**, 67A–76A. https://doi.org/10.1021/ac00238a765
57. N. I. Yanchenko and O. L. Yaskina, *Bull. Tomsk Polytech. Univ. Geo Assets Eng.*, 2014, **324**, 27–35 (in Russian).